Rock Mech Rock Eng (2012) 45:619–629
DOI 10.1007/s00603-011-0219-5

TECHNICAL NOTE

# Quantitative Measurements of Fracture Aperture and Directional Roughness from Rock Cores

**Bryan S. A. Tatone · Giovanni Grasselli**

Received: 20 August 2011 / Accepted: 27 December 2011 / Published online: 24 January 2012


**Keywords** Fracture roughness · Fracture aperture · 3D scanning · Rock mass characterization · Core logging

## 1 Introduction

The hydro-mechanical behavior of a blocky rock mass near the surface and at shallow depths is more dependent on the characteristics of the system of discontinuities within the rock mass than the characteristics of the intact rock. Discontinuities represent planes of weakness and conduits of enhanced hydraulic conductivity relative to the intact rock. The spatial aperture distribution and roughness of these fractures can have a significant influence on their hydro-mechanical behavior. In terms of mechanical behavior, the aperture distribution and roughness directly affect the spatial distribution and inclination of contact areas, which in turn influence the stress distribution, deformation, and asperity damage, under normal and shear loading (e.g., Re and Scavia 1999; Gentier et al. 2000; Grasselli and Egger 2003). In terms of hydraulic behavior, the spatial aperture distribution and roughness directly affect the tortuosity and connectivity of flow paths, which in turn influence the hydraulic transmissivity of the fracture (Zimmerman and Bodvarsson 1996; Berkowitz 2002).

The evaluation of fracture roughness requires measurements or observations of surface topography coupled with some empirical (e.g., Barton and Choubey 1977), statistical (e.g., Reeves 1985; Maerz et al. 1990) or fractal (e.g., Seidel and Haberfield 1995; Kulatilake et al. 2006) analysis methodologies, which yield one or more roughness parameters. Several contact and non-contact tools and techniques have been used to measure surface topography of discontinuity surfaces in rock. Contact techniques include:

1. *linear profiling methods*, such as stylus and roller profilometers (e.g., Weissbach 1978; Brown and Scholz 1985), profile combs (e.g., Barton and Choubey 1977; Stimpson 1982), straight edges and rulers (e.g., Piteau 1970; Milne et al. 1992) and shadow profilometry (Maerz et al. 1990); and
2. *local surface orientation methods*, such as the compass and disc-clinometer method (Fecker and Rengers 1971) and the equilateral tripod or connected pin methods (Rasouli and Harrison 2004).

Non-contact techniques include:

1. *passive or active triangulation methods*, such as structured light projection (e.g., Lanaro 2000; Hong et al. 2006; Tatone and Grasselli 2009a) and photogrammetry (Jessell et al. 1995; Lee and Ahn 2004; Baker et al. 2008); and
2. *distance measurement methods* such as laser scanning (e.g., Fardin et al. 2004; Renard et al. 2006; Sagy et al. 2007) and laser profilometry (e.g., Huang et al. 1992; Brown 1995; Kulatilake et al. 1995).

The measurement of the spatial distribution of fracture aperture also involves the measurement of the fracture surface topography. However, there is the added complexity of establishing the proper relative position of each fracture wall. Several methods have been developed to

B. S. A. Tatone · G. Grasselli (✉)
Department of Civil Engineering, University of Toronto, Toronto, Canada
e-mail: giovanni.grasselli@utoronto.ca

B. S. A. Tatone
e-mail: bryan.tatone@utoronto.ca

directly measure fracture aperture. These methods can be grouped into three categories:

1. *referenced contact or non-contact surface topography measurements* (e.g., Brown and Scholz 1985; Gentier et al. 1989; Lanaro 2000);
2. *injection or casting techniques* (e.g., Pyrak-Nolte et al. 1987; Hakami and Larsson 1996; Gentier and Hopkins 1997); and
3. *non-invasive techniques*, such as X-ray computed tomography (Johns et al. 1993; Keller 1998; Ketcham et al. 2010).

Although the above techniques can yield accurate descriptions of the fracture aperture geometry and roughness, they are each subject to varying limitations. Some techniques are restricted to laboratory use (i.e., immobile); some are destructive, meaning the fracture cannot be used for any other testing; some are limited in terms of the physical size of the fracture that can be characterized; and some are time-consuming, which limit the number and size of fracture specimens that can be measured at a given resolution. Table 1 attempts to provide a general comparison of which limitations apply to the categorized methods. It must be emphasized that this table represents a general qualitative assessment and that not all tools within a category may be subject to the same limitations.

As a result of these limitations, during drilling investigations, where many fractures must be logged, fracture aperture and roughness are typically assessed by more rapid methods. Often, the goal is to determine parameter values for rock mass classification systems [e.g., *Jr* in the NGI Q system (Barton et al. 1974), *condition of discontinuities* in the RMR system (Bieniawski 1989) and *surface condition* in the GSI system (Hoek et al. 1995)] or determine values of *JRC* to estimate discontinuity shear strength according to the Barton-Bandis shear strength criterion (Barton and Choubey 1977; Barton and Bandis 1990) or convert from mechanical to hydraulic apertures for fracture conductivity (Barton et al. 1985) and grout-take estimates (Barton 2004).

The above rock mass classification parameters are often based on qualitative observations of discontinuity surfaces, which can be made as core is logged. In contrast, *JRC* can be estimated by photographing a profile obtained with a profile comb and later comparing it to a set of standard profiles or measuring the ratio of the amplitude of surface roughness, $a$, to joint length, $L$, which is empirically related to *JRC* (Barton and Bandis 1990). The simplicity and rapid rate at which such parameters can be obtained is essential for logging hundreds of meters of core. However, these assessments are approximate and, without sufficient experience, can be subjective, biased and potentially lead to inaccurate discontinuity characterization and rock mass ratings (Beer et al. 2002).

The objective of this technical note is to describe a general method to obtain objective measurements of fracture aperture and oriented roughness from rock core through the digitization of fractures. An example of the application of the proposed method is then presented. For the example spatial data are acquired with a measurement system that employs a combination of active and passive triangulation to measure surface topography. These high-resolution measurements (nominal point spacing $<0.5$ mm) can be acquired in the field or laboratory on a large subset of the cored fractures to complement the typical assessments conducted as part of conventional geomechanical core logging. Compared to many other non-contact measurement systems (with sufficient accuracy and precision) used to measure fracture apertures, the advantage of this type of system is its ability to be used outside of a laboratory and the rate at which 3D point clouds can be acquired.

With oriented core, anisotropy in the roughness and spatial aperture distribution can be referenced to the true fracture orientation. These data can be subsequently used to

**Table 1** Relative comparison of fracture topography and fracture aperture measurement methods

| Method | Limitations | | | |
|---|---|---|---|---|
| | Physical size | Time to acquire data | Mobility | Destructive |
| *Fracture topography measurement* | | | | |
| Linear profiling | Some | High | Low | None |
| Local surface orientation | Some | High | Low | None |
| Non-contact triangulation | Low | Some | Low | None |
| Non-contact distance measurement | Low | Some | Low | None |
| *Aperture measurement* | | | | |
| Referenced topography measurements[a] | Some | None | None | None |
| Casting or injection techniques | Some | High | High | High |
| Non-invasive techniques | High | High | High | None |

[a] Here, it is assumed that the topography measurements have already been acquired

derive more reliable input parameters for hydro-mechanical modeling of the rock mass where only core-based data are available. For example, a FISH function for 3DEC (Itasca International Inc. 2011) could be developed to model shear strength as a function of the relative displacement vectors along fracture surfaces. In terms of hydraulic behavior, the Lattice-Boltzman Method (LBM) can be used to approximate the solution to the Navier–Stokes equations, while accounting for the actual spatial aperture distribution (Auradou et al. 2005; Boutt et al. 2006; Eker and Akin 2006; Basagaoglu et al. 2008). Hence, the influence of the fracture geometry on the flow path tortuosity and fracture transmissivity can be explicitly modeled, which is of interest to: petroleum and geothermal reservoir engineering, environmental remediation activities and underground nuclear waste disposal.

## 2 Method

### 2.1 Equipment

To measure the aperture distribution and roughness of a cored rock fracture sample, the corresponding 3D fracture surfaces must be digitized with a high-resolution (nominal point spacing of less than 500 μm) and high-precision measurement system (measurement noise not exceeding 5% of the point spacing). Several commercial non-contact measurement systems, based on structured light projection and laser scanning, that meet these specifications are now available. The system should be portable if it is to be used in the field environment. The example in Sect. 3 of this note considers one such measurement system.

### 2.2 Aperture Measurement

The measurement of fracture aperture requires the digitization of both fracture walls and knowledge of the relative position of each wall when the fracture is closed. These requirements are satisfied by first digitizing the external surface of the core sample with the fracture in a closed position (i.e., $\sigma_n = 0$) and then digitizing each fracture wall independently. In doing so, three digital models of the fracture sample are created. Multiple individual measurements may be required to obtain each of these three models depending on the setup of the measurement system. That is, measurements from different positions may be required to digitize the complete circumference of the core, since the entire surface cannot be viewed from a single position. When measuring the fracture in the closed position, it is advisable to reposition the measurement system rather than the specimen to avoid relative movement of the two core halves. When measuring the fracture walls, repositioning can be accomplished by moving either the specimen or measurement system.

Prior to digitization, reference points must be applied around the circumference of the core to transform individual measurements into a common coordinate system and to later transform each of the three models into a common coordinate system. Also, any reference line from oriented core drilling should be marked such that it can be distinguished in the 3D models. The location of this line is required to orient roughness measurements, as described in the following subsection. A piece of tape applied to the core that is aligned with the reference line can serve this purpose.

Following digitization, the digital models of the top and bottom of the fracture sample are rigidly transformed with respect to the model of the perimeter of the closed fracture using the reference points common to each model. In doing so, the top and bottom fracture walls are repositioned such that the closed position of the fracture under zero stress is replicated. The coordinate axes are then aligned such that the *xy*-plane defines the best-fit plane through the fracture surface with the positive *z*-axis directed upward and origin located on the core axis. The distance between the top and bottom fracture wall, measured perpendicular to the *xy*-plane, defines the fracture aperture. It should be noted that if the fracture plane displays a macroscopic curvature or steps, the best-fit plane through the fracture plane can be directionally biased. As a result, caution must be exercised when interpreting the aperture measurements.

The spatial aperture data can be displayed as a color map overlaid on the triangulated irregular network (TIN) surface or plotted as a 2D isopach map. In addition, the individual point measurements can be exported in an ASCII file (format: *x*, *y*, *z*, aperture) to produce plots of the relative frequency and cumulative probability distributions of the aperture. An example of an aperture color map and aperture distributions of a cored rock joint are shown in the example in Sect. 3 of this note.

### 2.3 Oriented Roughness Measurement

With each wall of the fracture surface digitized, the fracture surfaces can be cropped from the digital models to perform roughness analysis. A wide variety of statistical (e.g., Reeves 1985; Maerz et al. 1990) or fractal (e.g., Seidel and Haberfield 1995; Kulatilake et al. 2006) approaches can be employed to parameterize the fracture roughness. Both 2D parameters, based on the analysis of profiles, and 3D parameters, based on the analysis of surfaces, can be adopted. However, 3D parameters are preferred as 2D values based on profiles can lead to incomplete and biased roughness estimates (e.g., McWilliams et al. 1990; Riss and Gentier 1990; Rasouli and Harrison 2004).

Fracture roughness and, consequently, shear resistance are often anisotropic (Huang and Doong 1990; Jing et al. 1992; Aydan et al. 1996). This directional anisotropy in roughness is typically displayed using polar plots of roughness parameters obtained in different orientations. These parameters can be 2D parameters obtained from profiles oriented in different directions (Kulatilake et al. 1995; Haneberg 2007; Tatone and Grasselli 2010) or 3D parameters obtained by analyzing a fracture surface in different directions (Tatone and Grasselli 2009a). If one of the axes of the polar plots is aligned with the line of maximum dip on the fracture surface, the roughness in any direction on the fracture surface relative to the line of maximum dip can be read directly from the polar plot. To align the polar plot axes with the line of maximum dip, the $x$ or $y$ coordinate axis of the digital model of the fracture surface must be coincident with the line of maximum dip.

To find the line of maximum dip on a cored fracture surface, oriented core drilling techniques are required. Through these techniques, a reference line is marked on the core that is used to determine true discontinuity orientations. For inclined boreholes, a reference line is commonly marked at the lowermost point of the core called the bottom-of-hole (BOH) reference line. The BOH reference line marks the lowermost line of intersection between the borehole and a vertical plane containing the core axis. Looking down-hole along the core axis, the clockwise angle, measured about the core axis between the line of maximum dip and the BOH reference line, can be established using inclined stereographic analysis. As exemplified in Fig. 1a, the analysis proceeds as follows (after Priest 1985):

- First, plot the true orientation of the borehole and line of maximum dip for the true discontinuity on a lower hemispherical projection.
- Subsequently, rotate the borehole about an axis that is perpendicular to the borehole trend until the borehole and BOH reference line are vertical. At the same time, rotate the line of maximum dip about the same axis through an equal number of degrees.
- Finally, mark the trend of a vector that extends from the core axis to the BOH reference line on the perimeter of the hemispherical projection. Measure the clockwise angle around the circumference of the projection between this mark and the trend of the inclined line of maximum dip.

To further clarify, Fig. 1b–e describes the above procedure via 3D illustrations. Figure 1b is a plan view (i.e., top–down view) of a length of core and a discontinuity with the same orientations given in Fig. 1a. Figure 1c shows a plane view of the bottom half of the core with the line of maximum dip and BOH reference line indicated. Since the view

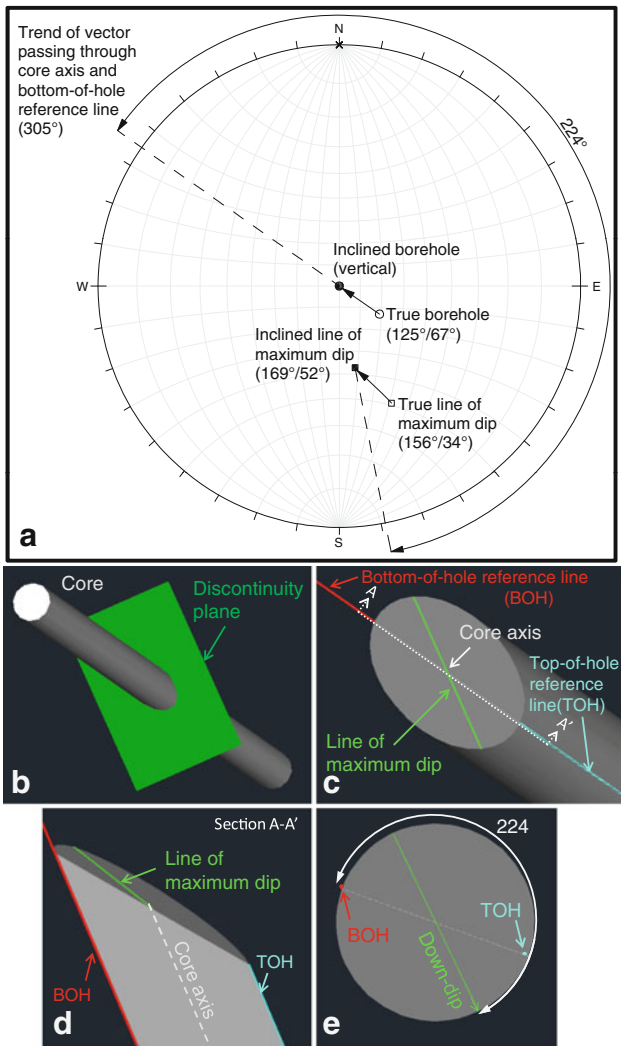


**Fig. 1** **a** Illustration of stereographic analysis used to find the line of maximum dip of fractures relative to the oriented core reference line; **b** 3D illustration showing *top–down view* of fracture plane and borehole; **c** *top–down view* of *bottom* fracture wall showing the bottom-of-hole reference line and line of maximum dip; **d** *vertical cross-sectional view* of the core along the core axis; **e** *top–down view* along the core axis showing measurement of angle between the reference line and *down-dip direction*

is again from the top–down, a vertical plane through the core axis appears as a straight line coincident with both the BOH and the TOH reference lines. From Fig. 1d, which is a cross section coincident with this vertical plane (Section A–A′), the BOH reference line is shown to be the lowermost line of intersection between the core and vertical plane. Lastly, Fig. 4d shows the same piece of core looking down the core axis (i.e., core is vertical) showing the clockwise angle between the BOH reference line and down-dip direction measured about the core axis.

A vector lying on the $xy$-plane (i.e., best-fit plane of the fracture surface) that extends from the core axis (0,0,0) to a

point on the perimeter of the core and is 224° clockwise from the BOH reference line (measured about the core axis) defines the orientation of the line of maximum dip on the fracture surface. By rotating about the previously defined $z$-axis, the $x$-axis or $y$-axis can be aligned with this line of maximum dip. With this rotation, the 0°–180° or 90°–270° axis of the roughness polar plot will coincide with the line of maximum dip. An example of oriented roughness analysis of a cored rock joint, in which the line of maximum dip is aligned with the 90°–270° axis of a polar plot, is given in Sect. 3 of this note.

It is noted that if many discontinuities are to be processed, the manual stereographic procedure described above may be too slow to be practical. In these situations, the same inclination of the borehole and line of maximum can be performed using the vector computations given in the algorithm of Priest (1983). This algorithm can be cast into a spreadsheet macro or MATLAB script to quickly determine the angle between the BOH reference line and line of maximum dip about the core axis for a series of discontinuities.

## 3 Example

Section 3 presents an example of the application of the method described above. The example considers a single discontinuity in a piece of core from an inclined borehole.

### 3.1 Measurement System

For this example, a 3D stereo-topometric measurement system (Advanced TOpometric Sensor (ATOS) II, manufactured by GOM mbH) was employed. The ATOS II system consists of a sensor head containing a central projector unit and two charge coupled device (CCD) cameras, along with a high-performance PC to pilot the system (dual 2.4 GHz AMD-Opteron processors, 16 gb ram). The system can be mounted on a boom to perform measurements in the laboratory with increased stability and positioning flexibility (Fig. 2a) or on a tripod for increased portability in field applications (Fig. 2b).

To digitize an object, the system projects a series of structured white-light fringe patterns onto the object's surface (Fig. 2c). Images of these patterns, which become distorted due to the relief of the surface, are automatically captured by the two CCD cameras. From these image pairs, the software automatically computes precise 3D coordinates for each pixel based on the principle of triangulation. With the CCD camera resolution of 1,392 × 1,040 pixels, a point cloud of up to 1.4 million surface points can be obtained in a single measurement. A single measurement can be acquired in 1–2 s depending on the selected shutter speed of the cameras. The acquired point cloud is subsequently polygonized into a triangulated irregular network (TIN) using a Delaunay triangulation scheme, whereby the measured points comprise the vertices of the TIN (Fig. 2d).

The average spacing between these points can be varied from 0.02 mm to 1.43 mm by changing the lenses of the CCD cameras and central projector, and varying the working distance and offset and angle between the two cameras. For this example, the ATOS system was configured to acquire points with a nominal spacing of 0.250 mm. The corresponding lens focal length, working distance and relative camera position are summarized in Table 2.

### 3.2 Aperture Distribution

As shown in Fig. 3a, the ATOS system was used to digitize the core in the closed position and each half of the core individually. In acquiring each of these digital models, multiple measurements with the system were required from different positions, as only points simultaneously visible in the left and right cameras are digitized in a single measurement. By affixing reference points around the edges of the fracture sample boundaries, which are uniquely identified according to their relative position, the ATOS software automatically transformed subsequent measurements into a common coordinate system. These same reference points were later used to transform the both digitized halves of the fracture into the closed position (Fig. 3b). In acquiring multiple measurements of the fracture in the closed position, it was the measurement system that was repositioned, and not the specimen to avoid relative movement of the fracture walls.

With the two digitized halves of the fracture transformed into a closed position, the distance between the two fracture walls was measured perpendicular to the $xy$-plane (i.e., the best-fit plane through the fracture surface). The aperture measurements were then plotted as a color map overlain on the lower fracture wall (Fig. 4a) and exported as an ASCII file (format: $x$, $y$, $z$, aperture) to allow the aperture distribution to be plotted (Fig. 4b).

The transformation of the fracture walls into the closed position, the creation of the best-fit plane through the fracture surface, and the measurement of the perpendicular distance between the fracture walls were all completed using the ATOS software v6.1.

### 3.3 Oriented Roughness

The application of ATOS systems[1] to measure rock fracture surfaces for roughness analysis has been previously

[1] http://www.gom.com/metrology-systems/system-overview/atos.html.


**Fig. 2** **a** and **b** ATOS II scanner by GOM setup for laboratory and in situ digitization, respectively; **c** example of fringe projection onto a fracture surface; **d** example of digital model of a fracture wall

**Table 2** Details of ATOS system configuration used in the example

| Parameter | Value |
|---|---|
| Lens focal length | 0.35 mm |
| Working distance | 1.03 m |
| Angle between cameras | 30° |
| Camera offset | 0.5 m |

demonstrated in several studies (Hong et al. 2006; Nasseri et al. 2009; Tatone 2009; Tatone and Grasselli 2009b). However, these studies either did not consider roughness anisotropy or considered anisotropy with respect to an arbitrary local coordinate system, without reference to the true fracture orientation.

Considering the 3D directional roughness parameterization of Tatone and Grasselli (2009a), Fig. 5a–c illustrates the cropping, rotation and alignment, and roughness polar plot for the lower wall of the example fracture, respectively. The 90° and 270° orientation of the roughness polar plot coincides with the up-dip (positive $y$-axis) and down-dip (negative $y$-axis) direction on the fracture surface, respectively. The line of maximum dip was defined following the approach presented in Sect. 2.2.

According to this roughness evaluation method, the roughness parameter, $\theta_{max}^*/[C + 1]$, characterizes the cumulative distribution of the apparent inclination of each triangular facet of the TIN surface in a selected direction. $\theta_{max}^*$ is the inclination of the steepest facet and $C$ is a fitting parameter that describes the shape of the cumulative

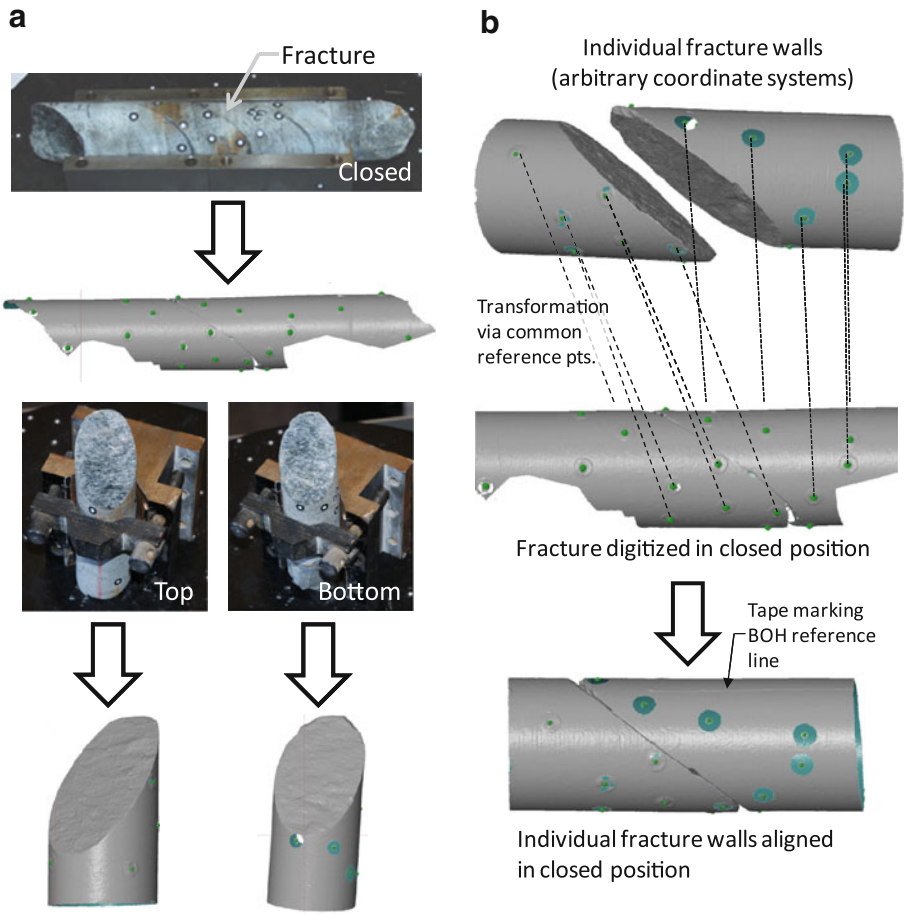


**Fig. 3** **a** Data acquisition procedure to measure fracture aperture; **b** transformation procedure to measure fracture aperture

distribution. A higher proportion of steeply inclined facets is indicative of a rougher surface and is reflected by a larger value of $\theta_{max}^*/[C+1]$. Further details regarding this particular roughness evaluation methodology are provided in Tatone and Grasselli (2009a).

### 3.4 Practicality

The key factors influencing the practicality of the above method are the ease at which the ATOS system can be used and transported in the field and the time required to analyze the data to obtain the aperture and roughness information.

To operate the ATOS system in the field, an alternating current (AC) power source is required. A 1000-watt portable generator or AC inverter attached to a site vehicle is sufficient for this purpose. Secondly, scanning must take place in a covered area to protect the system from the elements and avoid strong ambient lighting that can wash out the projected fringe patterns[2]. A 'sea can' core shack, typical of some drilling investigation programs, provides suitable protection from the elements and strong ambient lighting during scanning. During transportation to the next borehole location or drilling project, the system can be packed into its protective carrying case.

The time required to measure the aperture and roughness, according to the method described above, can be divided into the time required for raw data acquisition and the time required to process the raw data to obtain estimates of the aperture distribution and directional roughness. The data acquisition is all that is required in the field. The time required to prepare a cored fracture for scanning and complete all scanning was roughly 10 min. With this duration, scanning of every fracture quickly becomes impractical for cores from highly jointed rock masses. Thus, as mentioned previously, it is suggested that these types of measurements may be obtained from a subset of the total number of fractures encountered by the core.

The time required to process the data for each fracture following acquisition depends on the selected measurement resolution and, hence, raw data file sizes. Considering a single fracture digitized with nominal point spacing of 250 μm, the time needed to manually align, polygonize, analyze and export the results can vary from 10 to 15 min. However, the processing time per fracture can be reduced by batch processing the data acquired from multiple

[2] New technological developments in the latest version of the system allow it to acquire data regardless of ambient lighting conditions.

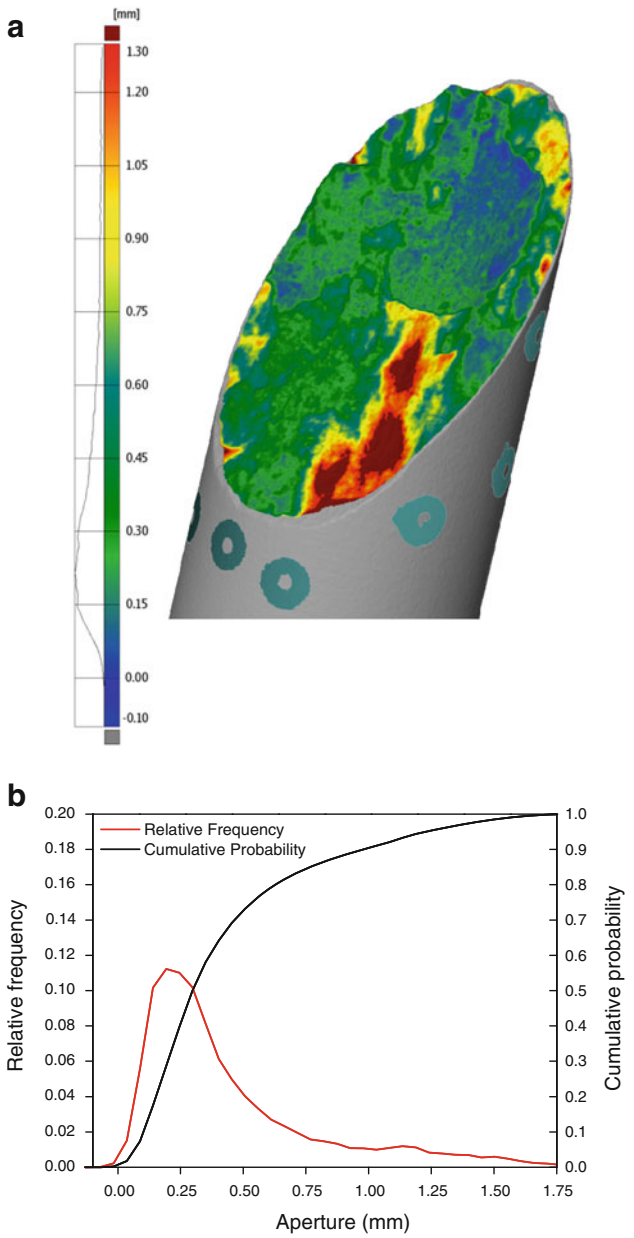


**Fig. 4** **a** Example of spatial aperture distribution as determined using the ATOS software; **b** example of relative frequency and cumulative distribution of fracture aperture

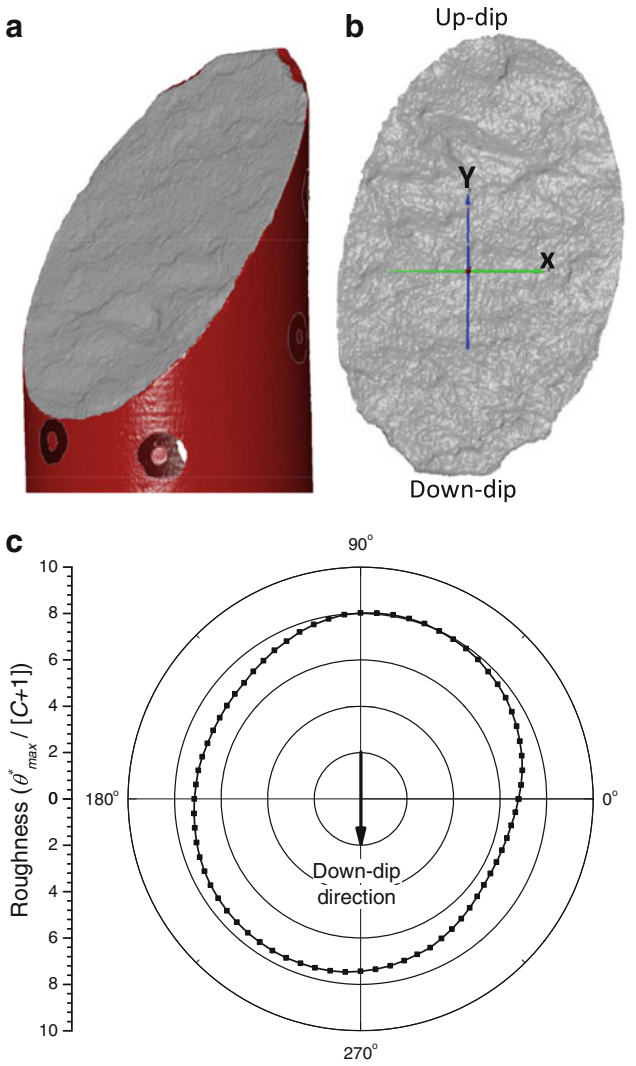


**Fig. 5** **a** Area to be cropped to perform roughness analysis; **b** cropped digital model of fracture surface aligned such that the *down-dip direction* is oriented *downward* and the best-fit plane through the surface is perpendicular to the *z*-axis; **c** results of 3D roughness analysis where the 270° direction corresponds with the *down-dip direction* on the fracture surface

fractures using scripts written in the Python-based[3] programming language within the ATOS software.

### 3.5 Benefits

Despite the added time needed to complete ATOS scanning of fractures in rock core, there are a number of benefits associated with acquiring such measurements. These benefits are as follows:

- Provides objective estimates of aperture and roughness that can be compared to the values of typical parameters that are rapidly estimated in the field (e.g., *Jr*, *condition of discontinuities, surface condition*) or those based on empirical relationships with measurements of *a/L* from photographs of roughness profiles (e.g., JRC). In doing so, the relative correctness of estimates can be ensured and any biases introduced by different field staff can be identified and addressed.
- Provides a permanent digital record of the fracture that could be assessed quantitatively or qualitatively at any time in the future.
- Provides directional roughness estimates that indicate potential anisotropy of shear strength. Such information

[3] http://www.python.org/.

has potential application in 3D numerical modeling of jointed rock masses, as shear strength can be defined as a function of the relative displacement vectors along fracture surfaces.
- Provides physical limits for coupled hydro-mechanical modeling of flow in rock fractures. It has been shown that irregular and anisotropic surface topography can lead to complex recirculation patterns and flow channeling (e.g., Iwai 1976; Tsang 1984; Brown 1987; Tsang and Tsang 1989, among others).

### 3.6 Measurement Accuracy

For the examples shown in Figs. 4 and 5, measurement points were obtained on a nominal 250 μm *xy* grid with measurement noise no greater than 10 μm. With this particular setup, the measurement volume (i.e., 3D field of view) of the system was 350 × 280 × 280 $mm^3$. With this volume, each wall of a cored fracture sample can be digitized with two to four individual measurements. Although a finer resolution with less noise can be achieved, the measurement volume is decreased in doing so. Thus, several additional individual measurements, and consequently time, would be required to digitize both fracture walls.

In addition to measurement noise, the transformation of each fracture wall into its closed position has an associated error. Upon transformation, the ATOS system minimized the error between the common reference points in the reference object (i.e., fracture digitized in closed position) and the object being transformed (i.e., digitized fracture wall) and reports the minimized mean deviation. With the ATOS setup to acquire points at a nominal spacing of 250 μm, mean reference point deviations are typically between 10 and 20 μm. The combined three-dimensional error and its influence on roughness and aperture measurements are difficult to quantify. However, some important notes regarding accuracy and approximate estimates of the resulting error in roughness and aperture estimates can be made:

- The percent error in aperture and roughness estimates depends on the degree of fracture roughness and openess, respectively. For example, assuming that 10–20 μm transformation error results in a 10–20 μm error in aperture (a worst case scenario), a fracture with a mean aperture of 500 μm will contain 2–4% error. Yet, a fracture with a mean aperture of only 50 μm will have a 20–40% error.
- Assuming the cubic law applies for flow in the fracture of unit width, the fracture transmissivity, $T$, is given as $T = h^3/12$, where $h$ is the aperture (Zimmerman and Bodvarsson 1996). Hence, the error related to the aperture measurements is cubed when considering the transmissivity. Considering the above hypothetical fractures with mean apertures of 500 μm (2–4% error) and 50 μm (20–40% error), the resulting error in transmissivity estimates are 6–13 and 49–175%, respectively.
- Assuming the noise level of 10 μm results in two adjacent points (250 μm apart) being, +10 μm and −10 μm above and below their true positions (again, a worst case scenario), an error in slope of roughly ±2.3° would result. For a roughness evaluation method based on the slope of individual asperities (as in this note), this small variation is essentially inconsequential to the estimated roughness as fractures typically show a much larger range of asperity slopes.
- In contrast to the noise, the measurement resolution has a significant effect on all roughness parameters. For this reason, the selected resolution chosen by the user should be sufficiently fine to capture the geometry of features of the surface that are involved in the shearing process. Furthermore, the resolution of the measurements must be consistent to permit comparison of roughness metrics (Tatone et al. 2010).

## 4 Conclusion

This paper has presented a method to measure directional fracture roughness and the spatial aperture distribution under zero normal stress of fractures in rock cores. The method makes use of high-resolution 3D surface measurements such as those that can be obtained with a portable stereo-topometric camera. It is proposed that the method can be applied to a large subset of cored fractures at the drilling location without adding a significant amount of effort to conventional geomechanical core logging procedures. The objective data obtained according to this method allows the consistency of typical qualitative assessments to be checked, provides a digital record of fractures that can be accessed at any time in the future, provides reference of roughness anisotropy to the true discontinuity orientation, and provides geometric data for hydro-mechanical modeling that are usually not available. Thus, the proposed method is considered an important step in moving forward from subjective assessments to quantitative and objective measurements of roughness and aperture distribution in rock core.

**Acknowledgments** This work has been supported by the Natural Science and Engineering Research Council of Canada in the form of Discovery Grant No. 341275 and RTI Grant No. 345516 held by G. Grasselli and by an OGSST Graduate Scholarship held by B.S.A. Tatone.

## References


Auradou H, Drazer G, Hulin JP, Koplik J (2005) Permeability anisotropy induced by the shear displacement of rough fracture walls. Water Resour Res 41(9):W09423

Aydan Ö, Shimizu Y, Kawamoto T (1996) The anisotropy of surface morphology characteristics of rock discontinuities. Rock Mech Rock Eng 29(1):47–59

Baker BR, Gessner K, Holden E-J, Squelch AP (2008) Automatic detection of anisotropic features on rock surfaces. Geosph 4(2):418–428

Barton N (2004) The theory behind high pressure grouting. Tunn Tunn Int, Part 1, Sept., pp 28–30, Part 2, Oct., pp 33–35

Barton N, Bandis S (1990) Review of predictive capabilities of JRC-JCS model in engineering practice. In: Barton N, Stephansson O (eds) Rock Joints; Proceedings of the International Symposium on Rock Joints, Loen, Norway, 4–6 June 1990. A. A Balkema, Rotterdam, pp 603–610

Barton N, Choubey V (1977) The shear strength of rock joints in theory and practice. Rock Mech Rock Eng 10(1):1–54

Barton N, Lien R, Lunde J (1974) Engineering classification of rock masses for the design of tunnel support. Rock Mech Rock Eng 6(4):189–236

Barton N, Bandis S, Bakhtar K (1985) Strength, deformation and conductivity coupling of rock joints. Int J Rock Mech Min Sci Geomech Abstr 22(3):121–140

Basagaoglu H, Meakin P, Succi S, Redden GR, Ginn TR (2008) Two-dimensional lattice Boltzmann simulation of colloid migration in rough-walled narrow flow channels. Phys Rev E 77(3):031405

Beer AJ, Stead D, Coggan JS (2002) Estimation of the joint roughness coefficient (JRC) by visual comparison. Rock Mech Rock Eng 35(1):65–74

Berkowitz B (2002) Characterizing flow and transport in fractured geological media: a review. Adv Water Resour 25(8–12):861–884

Bieniawski ZT (1989) Engineering rock mass classifications. Wiley, New York

Boutt DF, Grasselli G, Fredrich JT, Cook BK, Williams JR (2006) Trapping zones: the effect of fracture roughness on the directional anisotropy of fluid flow and colloid transport in a single fracture. Geophys Res Lett 33(21):L21402

Brown SR (1987) Fluid flow through rock joints: the effect of surface roughness. J Geophys Res 92((B2)):1337–1347

Brown SR (1995) Simple mathematical model of a rough fracture. J Geophys Res 100(B4):5941–5952

Brown SR, Scholz CH (1985) Broad bandwidth study of the topography of natural rock surfaces. J Geophys Res 90(B14): 2575–2582

Eker E, Akin S (2006) Lattice boltzmann simulation of fluid flow in synthetic fractures. Transp Porous Media 65(3):363–384

Fardin N, Feng Q, Stephansson O (2004) Application of a new in situ 3D laser scanner to study the scale effect on the rock joint surface roughness. Int J Rock Mech Min Sci 41(2):329–335

Fecker E, Rengers N (1971) Measurement of large scale roughness of rock planes by means of profilograph and geological compass. In: Proceedings of the Symposium on Rock Fracture, Nancy, France, 1971, pp 1–18

Gentier S, Hopkins DL (1997) Mapping fracture aperture as a function of normal stress using a combination of casting, image analysis and modeling techniques. Int J Rock Mech Min Sci 34(3–4):132.e1–132.e14

Gentier S, Billaux D, van Vliet L (1989) Laboratory testing of the voids of a fracture. Rock Mech Rock Eng 22(2):149–157

Gentier S, Riss J, Archambault G, Flamand R, Hopkins DL (2000) Influence of fracture geometry on shear behavior. Int J Rock Mech Min Sci 37(1–2):161–174

Grasselli G, Egger P (2003) Constitutive law for the shear strength of rock joints based on three-dimensional surface parameters. Int J Rock Mech Min Sci 40(1):25–40

Hakami E, Larsson E (1996) Aperture measurements and flow experiments on a single natural fracture. Int J Rock Mech Min Sci Geomech Abstr 33(4):395–404

Haneberg W (2007) Directional roughness profiles from three-dimensional photogrammetric or laser scanner point clouds. In: Eberhardt E, Stead D, Morrison T (eds) Rock Mechanics: Meeting Society's Challenges and Demands; proceedings of the 1st Canada-US rock mechanics symposium, Vancouver, Canada, 27–31 May 2007. Taylor and Francis, London, pp 101–106

Hoek E, Kaiser PK, Bawden WF (1995) Support of Underground Excavations. A. A Balkema, Rotterdam

Hong ES, Lee IM, Lee JS (2006) Measurement of rock joint roughness by 3D scanner. Geotech Test J 29(6):482–489

Huang TH, Doong YS (1990) Anisotropic shear strength of rock joints. In: Barton N, Stephansson O (eds) Rock Joints, Loen, Norway, 4–6 June 1990. Balkema, Rotterdam, pp 211–218

Huang SL, Oelfke SM, Speck RC (1992) Applicability of fractal characterization and modelling to rock joint profiles. Int J Rock Mech Min Sci Geomech Abstr 29(2):89–98

Itasca International Inc (2011) 3DEC. http://www.itascacg.com/3dec/overview.php. Accessed 12 Dec 2011

Iwai K (1976) Fundamental Studies of the Fluid Flow Through a Single Fracture. PhD., University of California, Berkeley

Jessell MW, Cox SJD, Schwarze P, Power WL (1995) The anisotropy of surface roughness measured using a digital photogrammetric technique. Geol Soc Lond Spec Publ 92(1):27–37

Jing L, Nordlund E, Stephansson O (1992) An experimental study on the anisotropy and stress-dependency of the strength and deformability of rock joints. Int J Rock Mech Min Sci Geomech Abstr 29(6):535–542

Johns RA, Steude JS, Castanier LM, Roberts PV (1993) Nondestructive measurements of fracture aperture in crystalline rock cores using X-ray computed tomography. J Geophys Res 98(B2): 1889–1900

Keller A (1998) High resolution, non-destructive measurement and characterization of fracture apertures. Int J Rock Mech Min Sci 35(8):1037–1050

Ketcham RA, Slottke DT, Sharp JM (2010) Three-dimensional measurement of fractures in heterogeneous materials using high-resolution X-ray computed tomography. Geosph 6(5):499–514

Kulatilake PHSW, Shou G, Huang TH, Morgan RM (1995) New peak shear strength criteria for anisotropic rock joints. Int J Rock Mech Min Sci Geomech Abstr 32(7):673–697

Kulatilake PHSW, Balasingam P, Park J, Morgan RM (2006) Natural rock joint roughness quantification through fractal techniques. Geotech Geol Eng 24(5):1181–1202

Lanaro F (2000) A random field model for surface roughness and aperture of rock fractures. Int J Rock Mech Min Sci 37(8): 1195–1210

Lee H-S, Ahn K-W (2004) A prototype of digital photogrammetric algorithm for estimating roughness of rock surface. Geosci J 8(3):333–341

Maerz NH, Franklin JA, Bennett CP (1990) Joint roughness measurement using shadow profilometry. Int J Rock Mech Min Sci Geomech Abstr 27(5):329–343

McWilliams PC, Kerkering JC, Miller SM (1990) Fractal characterization of rock fracture roughness for estimating shear strength. In: Rossmanith HP (ed) Mechanics of Jointed and Faulted Rock, Vienna, 18–20 April 1990. A.A Balkema, Rotterdam, pp 331–336

Milne D, Germain P, Potvin Y (1992) Measurement of rock mass properties for mine design. In: Hudson JA (ed) Proceedings of

the ISRM symposium on Rock Characterization: Eurock '92, Chester, England, 1992. Thomas Telford, London, pp 245–250

Nasseri MHB, Tatone BSA, Grasselli G, Young R (2009) Fracture toughness and fracture roughness interrelationship in thermally treated Westerly granite. Pure and Appl Geophys 166(5):801–822

Piteau DR (1970) Geological factors significant to the stability of slopes cut in rock. In: van Rensburg PWJ (ed) Proceedings of the Symposium on Planning Open Pit Mines, Johannesburg, South Africa, 1970. A.A Balkema, Rotterdam, pp 33–53

Priest SD (1983) Computer generation of inclined hemisphere projections. Int J Rock Mech Min Sci Geomech Abstr 20(1): 43–47

Priest SD (1985) Hemispherical Projection Methods in Rock Mechanics. George Allan and Unwin, London

Pyrak-Nolte LJ, Myer LR, Cook NGW, Witherspoon PA (1987) Hydraulic and mechanical properties of natural fractures in low permeability rock. In: Herget G, Vongpaisal S (eds) Proceedings of the 6th International Congress of Rock Mechanics, Montreal, 1987. A.A Balkema, Rotterdam, pp 225–232

Rasouli V, Harrison JP (2004) A comparison of linear profiling and an in-plane method for the analysis of rock surface geometry. Int J Rock Mech Min Sci 41(3):377–378

Re F, Scavia C (1999) Determination of contact areas in rock joints by X-ray computer tomography. Int J Rock Mech Min Sci 36(7):883–890

Reeves MJ (1985) Rock surface roughness and frictional strength. Int J Rock Mech Min Sci Geomech Abstr 22(6):429–442

Renard F, Voisin C, Marsan D, Schmittbuhl J (2006) High resolution 3D laser scanner measurements of a strike-slip fault quantify its morphological anisotropy at all scales. Geophys Res Lett 33:L04305

Riss J, Gentier S (1990) Angularity of a natural rock fracture. In: Rossmanith HP (ed) Mechanics of Jointed and Faulted Rock, Vienna, 18–20 April 1990. A.A Balkema, Rotterdam, pp 399–406

Sagy A, Brodsky EE, Axen GJ (2007) Evolution of fault-surface roughness with slip. Geology 35(3):283–286

Seidel JP, Haberfield CM (1995) Towards an understanding of joint roughness. Rock Mech Rock Eng 28(2):69–92

Stimpson B (1982) A rapid field method for recording joint roughness profiles. Int J Rock Mech Min Sci Geomech Abstr 19(6): 345–346

Tatone BSA (2009) Quantitative Characterization of Natural Rock Discontinuity Roughness In situ and in the Laboratory. MASc., University of Toronto, Toronto, Canada

Tatone BSA, Grasselli G (2009a) A method to evaluate the three-dimensional roughness of fracture surfaces in brittle geomaterials. Rev Sci Instrum 80(12), paper no. 125110

Tatone BSA, Grasselli G (2009) Use of a stereo-topometric measurement system for the characterization of rock joint roughness in situ and in the laboratory. In: Diederichs MS, Grasselli G (eds) Rock Engineering in Difficult Conditions; Proceedings of 3rd Canada-US Rock Mechanics Symposium, Toronto, Canada, 9–15 May 2009b, p 4145

Tatone BSA, Grasselli G (2010) A new 2D discontinuity roughness parameter and its correlation with JRC. Int J Rock Mech Min Sci 47(8):1391–1400

Tatone BSA, Grasselli G, Cottrell B (2010) Accounting for the influence of measurement resolution on discontinuity roughness estimates. In: Eurock 2010: Rock Mechanics in Civil and Environmental Engineering, Lausanne, Switzerland, 15–18 June 2010. A.A. Balkema, Rotterdam, pp 203–206

Tsang YW (1984) The effect of tortuosity on fluid flow through a single fracture. Water Resour Res 20(9):1209–1215

Tsang YW, Tsang CF (1989) Flow channeling in a single fracture as a two-dimensional strongly heterogeneous permeable medium. Water Resour Res 25(9):2076–2080

Weissbach G (1978) A new method for the determination of the roughness of rock joints in the laboratory. Int J Rock Mech Min Sci Geomech Abstr 15(3):131–133

Zimmerman RW, Bodvarsson GS (1996) Hydraulic conductivity of rock fractures. Transp Porous Media 23(1):1–30